Optimal nudging strategies in regional climate modelling: investigation in a Big-Brother experiment over the European and Mediterranean regions

Hiba Omrani · Philippe Drobinski ·
Thomas Dubos

Abstract The objective of this work is to gain a general insight into the key mechanisms involved in the impact of nudging on the large scales and the small scales of a regional climate simulation. A "Big Brother experiment" (BBE) approach is used where a "reference atmosphere" is known, unlike when regional climate models are used in practice. The main focus is on the sensitivity to nudging time, but the BBE approach allows to go beyond a pure sensitivity study by providing a reference which model outputs try to approach, defining an optimal nudging time. Elaborating upon previous idealized studies, this work introduces key novel points. The BBE approach to optimal nudging is used with a realistic model, here the weather research and forecasting model over the European and Mediterranean regions. A winter simulation (1 December 1989–28 February 1990) and a summer simulation (1 June 1999–31 August 1999) with a 50 km horizontal mesh grid have been performed with initial and boundary conditions provided by the ERA-interim reanalysis of the European Center for Medium-range Weather Forecast to produce the "reference atmosphere". The impacts of spectral and indiscriminate nudging are compared all others things being equal and as a function of nudging time. The impact of other numerical parameters, specifically the domain size and update frequency of the large-scale driving fields, on the sensitivity of the optimal nudging time is investigated. The nudged simulations are also compared to non-nudged simulations. Similarity between the reference and the simulations is evaluated for the surface temperature,

surface wind and for rainfall, key variables for climate variability analysis and impact studies. These variables are located in the planetary boundary layer, which is not subject to nudging. Regarding the determination of a possible optimal nudging time, the conclusion is not the same for indiscriminate nudging (IN) and spectral nudging and depends on the update frequency of the driving large-scale fields τ_a. For IN, the optimal nudging time is around $\tau = 3$ h for almost all cases. For spectral nudging, the best results are for the smallest value of τ used for the simulations ($\tau = 1$ h) for frequent update of the driving large-scale fields (3 and 6 h). The optimal nudging time is 3 for 12 h interval between two consecutive driving large-scale fields due to time sampling errors. In terms of resemblance to the reference fields, the differences between the simulations performed with IN and spectral nudging are small. A possible reason for this very similar performance is that nudging is active only above the planetary boundary layer where small-scale features are less energetic. As expected from previous studies, the impact of nudging is weaker for a smaller domain size. However the optimal nudging time itself is not sensitive to domain size. The proposed strategy ensures a dynamical consistency between the driving field and the simulated small-scale field but it does not ensure the best "observed" fine scale field because of the possible impact of incorrect driving large-scale field. This type of downscaling provides an upper bound on the skill possible for recent historical past and twenty-first century projections. The optimal nudging strategy with respect to dynamic downscaling could add skill whenever the parent global model has some level of skill.

H. Omrani (✉) · P. Drobinski · T. Dubos
Laboratoire de Météorologie Dynamique, Institut Pierre Simon Laplace, CNRS and Ecole Polytechnique, 91128 Palaiseau Cedex, France
e-mail: hiba.omrani@lmd.polytechnique.fr

1 Introduction

Dynamical downscaling has been widely used to produce regional climate description at fine scales (e.g. Hewitson and Crane 1996). With dynamical downscaling, a regional climate model (RCM) is driven at its boundaries by large-scale fields provided by analysis, reanalysis or a global climate model (GCM). The RCM is then expected to simulate high resolution physical processes consistent with the prescribed large scale weather evolution.

RCMs can be of different types. They can be a GCM with grid refinement over a specific region. The refinement can be done using a mesh stretching technique (e.g. Hourdin et al. 2006) or by moving the model pole over the region of interest (e.g. Déqué and Piedelievre 1995). RCMs can also be a limited area model (LAM). LAMs were originally developed for process studies at fine scale over meteorological time scales (few days simulation; e.g. Lebeaupin-Brossier and Drobinski 2009). With increasing computer resources, their use have been extended to regional climate modeling (e.g. Crétat et al. 2012; Flaounas et al. 2012a).

Both GCMs and LAMs are sensitive to the resolution and the content of physical parametrizations (Seth and Giorgi 1998; von Storch et al. 2000; Giorgi and Bi 2000; Alexandru et al. 2009; Crétat et al. 2012). Regarding LAMs specifically, previous studies have investigated the specific sensitivity of the predictions to the update frequency of the boundary conditions, the size and resolution of the domain of simulation in order to prevent these models to mislead (Bhaskaran et al. 1996; Noguer et al. 1998; Seth and Giorgi 1998; Denis et al. 2002, 2003; Castro et al. 2005).

In the context of regional climate modeling, long-term simulations of typically few decades have to be performed. Lo et al. (2008) showed that continuous runs can produce very low score when the simulations are compared to observations and that simulations re-initialised periodically have better results than continuous runs. However re-initialization creates discontinuities which are detrimental for time variability studies. All these studies have shown that RCMs possess an internal variability with a far from negligible impact on regional climate predictions.

One way to reduce internal variability is to apply large-scale nudging. This technique consists in partially imposing the large scale of the driving fields (DF) on the RCM simulation with the aim of disallowing large and unrealistic departures between driving and driven fields. Two different types of nudging exist: indiscriminate nudging which consists in relaxing the RCM's prognostic variables towards the GCM values within a predetermined relaxation time (e.g. Davies and Turner 1977; Salameh et al. 2010; Omrani et al. 2012a) and spectral nudging which consists

in driving the RCM on selected spatial scales (e.g. Waldron et al. 1996; von Storch et al. 2000; Radu et al. 2008; Omrani et al. 2012b). IN is also referred to as data assimilation, dynamical or Newtonian relaxation, grid-point nudging or analysis nudging (Davies and Turner 1977; Stauffer and Seaman 1994; Lo et al. 2008; Salameh et al. 2010; Omrani et al. 2012a). Both nudging techniques require the definition of a relaxation time controlling the nudging strength, with no obvious physical basis (e.g. Stauffer and Seaman 1990; Radu et al. 2008). A theoretical and practical issue is how the choice of this relaxation time affects the quality of the model outputs, and which values of the relaxation time are to be preferred.

This specific issue has been partially addressed using idealized numerical frameworks. In Salameh et al. (2010), the impact of IN on regional climate modeling has been investigated using a toy model consisting in resolving a linear transport equation with a Newtonian relaxation term. The toy model suffers from the same drift phenomenon as a complex atmospheric model and needs to be nudged as well. Salameh et al. (2010) consider the impact of the nudging time on the root-mean-square error of the modelled small and large scales. They predict the existence of an optimal nudging time minimizing the total error which depends on the time scale over which numerical errors affect significantly the accuracy of the solution at the large spatial scales, and the typical time scale of the small-scale phenomena that are not resolved in the coarse-resolution DF. However, since the toy model is linear, its drift is solely due to accumulating numerical errors and not to a genuine unpredictability. To overcome this limitation, Omrani et al. (2012a, b) have used a two-layer quasi-geostrophic (QG) model which presents more similarities to atmospheric dynamics. They used a "Big-Brother experiment" (BBE) approach, where a reference atmospheric state is known (Denis et al. 2002; De Elia et al. 2002) and investigated the impact on the QG internal variability of IN (Omrani et al. 2012a) and spectral nudging (Omrani et al. 2012b). They investigated the link between nudging and atmospheric predictability, numerical domain size, model resolution, and update frequency of the driving large-scale fields. In Omrani et al. (2012a), it has been shown that for IN, there is a trade-off between the adverse effect of nudging on small scales and the departure of the large-scales from the DF. This trade-off defines an optimal nudging time for which the small scales produced by the RCM are best correlated with a reference field. For a small domain, the boundary conditions sufficiently control the atmospheric dynamics and low sensitivity is found on the nudging time. Omrani et al. (2012b) showed that in spectral nudging, this trade-off does not exist since small scales are not affected. Contrary to expectations, an infinitely strong spectral nudging does not produce optimal

reconstruction of the small scales. Indeed, this would be true only if the DF were fully resolved in time. In fact they are typically sampled at intervals of a few hours, potentially undersampling smaller-scale phenomena that tend to evolve more rapidly. A consequence is that care must be given to the spatial resolution of the DF to ensure that they are adequately time-resolved. Omrani et al. (2012b) proposed a practical means to check that the forcing fields are adequately time-resolved and degrade their spatial resolution as necessary.

Of course, the simple nature of the QG model does not allow to transpose straightforwardly the results to real regional modelling. However, the use of dimensionless parameters in Omrani et al. (2012a, b) gives a methodology to evaluate with a realistic RCM how to realize the potential benefit of nudging as a function of other numerical parameters, here mainly the domain size and the frequency of update of boundary conditions. The RCM used in this study is the weather and research forecasting (WRF) LAM (Skamarock and Klemp 2007). Compared to the QG model used in Omrani et al. (2012a, b) the WRF model approaches much better the full complexity of the atmospheric processes. Compared to previous studies examining the sensitivity of RCM results to domain size and the frequency of update of boundary conditions (e.g. Bhaskaran et al. 1996; Noguer et al. 1998; Seth and Giorgi 1998; Denis et al. 2002; Denis et al. 2003; Castro et al. 2005), we address here specifically the interaction between these parameters and the nudging parameters. Previous studies have investigated nudging impact on regional climate simulations. For instance Castro et al. (2005) studied the sensitivity of RAMS model simulations to domain size and also to the activation of IN but a single large value of the nudging time (24 h) was considered. Rockel et al. (2008) compared spectrally nudged CLM simulations to the RAMS simulations of Castro et al. (2005) but the models themselves differed in many ways (dynamical core, physics package) so the comparison was not all other things being equal. Liu et al. (2012) compared spectral and IN in a common configuration of the WRF model but a single, small value of the nudging time (1 h) was used, which could be unfair to IN. Compared to these studies, we isolate the effect of nudging without any interference with other sources of error and uncertainty propagation, by using a BBE approach, meaning that the same model and hence the same physics are used. This investigation is based on an evaluation of the actual benefit of using nudging, indiscriminate or spectral, for the simulated variables of greatest importance for regional climate modeling (surface temperature, wind fields and rainfall). We compare the two nudging techniques, indiscriminate and spectral, because both techniques were widely used in previous studies. Furthermore, it would be interesting to identify configurations for which the simpler IN produces results with comparable quality as spectral nudging.

Key novel points of our work, elaborating upon previous idealized studies (Omrani et al. 2012a, b), are

- the use of a BBE approach which allows the determination of a possible optimal nudging time for a realistic model
- the determination of a possible optimal nudging time for both spectral and IN all others things being equal
- the examination of the impact of other numerical parameters, specifically the domain size and update frequency of the large-scale DF, on the sensitivity of optimal nudging time, as performed in Omrani et al. (2012a, b) with a QG model.

This study is of particular relevance in the context of the CORDEX program (cordinated downscaling experiment; Giorgi et al. 2009) endorsed by the world climate research program (WCRP). CORDEX aims at developing a framework to evaluate and possibly improve dynamical and statistical downscaling techniques for use in downscaling global climate projections. It also aims at fostering an international coordinated effort to produce improved multi-model downscaling-based high- resolution climate-change information over regions worldwide for input to impact / adaptation work and promoting greater interaction and communication between global climate modellers, the downscaling community and end-users to better support impact/adaptation activities. Our study focus on the first objective of CORDEX, i.e. evaluating and improving dynamical downscaling technique. In order to address the issue of the domain size, two CORDEX domains have been used: the EURO–CORDEX domain over Europe and the HyMeX/MED–CORDEX over the Mediterranean domain. The HyMeX/MED–CORDEX is a joint initiative between the hydrological cycle in the Mediterranean experiment (HyMeX; see international science plan on http://www.hymex.org and Drobinski et al. 2009a, b, 2010, 2011) and the CORDEX international programs for the specific investigation of the Mediterranean climate. These two domains overlap significantly and thus the results can be compared over the common domain.

This paper is organized as follows. A description of the model and the experiment set-up is given in Sect. 2 The impact of nudging on the WRF skill at reproducing the reference fields over Europe is investigated in Sect. 3 The comparison of the results obtained over the European and Mediterranean domains is discussed in Sect. 4. Finally, Sect. 5 summarizes the results and points out some open research questions needing further investigation.

2 Numerical setup

2.1 Model description

The model used in this study is the updated version 3.1.1 of the WRF model released on July 31, 2009. WRF is a LAM, non-hydrostatic, with terrain following eta-coordinate mesoscale modeling system designed to serve both operational forecasting and atmospheric research needs (Skamarock and Klemp 2007). The WRF development is a collaborative partnership, principally among the National Center for Atmospheric Research (NCAR), the National Oceanic and Atmospheric Administration (the National Centers for Environmental Prediction (NCEP) and the Forecast Systems Laboratory (FSL), the Air Force Weather Agency (AFWA), the Naval Research Laboratory, the University of Oklahoma, and the Federal Aviation Administration (FAA).

We use the physical options chosen to perform the HyMeX/MED–CORDEX simulations (Lebeaupin-Brossier et al. 2011, 2012a, b, c; Flaounas et al. 2012a). These include the WRF single-moment 5-class microphysical parameterization (Hong and Zhao 1998; Hong et al. 2004), the new Kain–Fritsch convective parameterization (Kain 2004), the Dudhia shortwave radiation (Dudhia 1989) and rapid radiative transfer model longwave radiation (Mlawer et al. 1997) and the Yonsei University planetary boundary layer scheme (Noh et al. 2003). For the land surface model (LSM), a 5-layer diffusive scheme is used here but other simulations are available with the rapid update cycle scheme (Flaounas et al. 2012a). In the context of HyMeX/ MED–CORDEX, ocean/atmosphere coupled simulations have also been performed using WRF with such configuration (Drobinski et al. 2012; Claud et al. 2012; Lebeaupin Brossier et al. 2012c).

In this work we use the BBE (Denis et al. 2002) to investigate the impact of the indiscriminate and spectral nudging on WRF skills to produce significant small scales from low resolution driving data. It consists in first establishing a reference climate by performing a large-domain high-resolution RCM simulation: this simulation is called the Big-Brother (BB). This reference simulation is then degraded by filtering short scales that are generally unresolved by the DF (e.g. global reanalysis and GCMs). This filtered reference is then used to drive the same nested RCM (called the Little-Brother LB), integrated at the same high-resolution as the Big Brother, but over a smaller domain that is embedded in the BB domain. The resemblance between LB and BB over the LB domain is characterized in terms of seasonal and spatial statistics : standard deviation of LB and of BB, mean bias, root-mean-square difference and correlation between LB and BB (Fig. 1). Differences can thus be attributed easily to errors associated with the nesting and downscaling technique, and not to model errors nor to observation limitations.

2.2 Nudging

We investigate the two existing nudging techniques, i.e. the IN and the spectral nudging (SN). The IN technique has been originally developed for assimilation purposes (Davies and Turner 1977; Schraff 1997; Yong et al. 1998; Vidard et al. 2003) but is increasingly popular to drive RCMs (Flaounas et al. 2012a, b) . The nudging technique consists in relaxing the model state towards the driving large-scale fields by adding a non-physical term to the model equation. This nudging term is defined as the difference between the observation and the model solution weighted by a nudging coefficient which is the inverse of the nudging time. In WRF, IN is represented by the general following equation [Eq. (1)].

$$\partial_t q_{LB} = F(q_{LB}) - \frac{1}{\tau}[q_{LB} - q_{DF}] \qquad (1)$$

where q is a prognostic variable. The subscripts DF and LB stand for driving field and LB, respectively. In WRF, IN can be applied to the wind components u and v (zonal and meridional wind components, respectively), to the potential temperature θ, and to the water vapor mixing ratio qv. The models physical forcing terms (advection, Coriolis effects, etc.) are represented by $F(.)$. The quantity $1/\tau$ is the nudging coefficient, with τ a representative time scale for the artificial nudging term. Following Lo et al. (2008), the two nudging techniques are applied only above a time-dependent planetary boundary layer height diagnosed by the planetary boundary layer scheme. Above that height the nudging coefficient is constant. For IN, the smaller the nudging time τ, the closer the RCM predictions q_{LB} to the driving large scale fields fields q_{DF} interpolated on the RCM grid and the larger the inhibition of the RCM physics. In this work, the nudging time is the same for all the nudged variables.

The spectral nudging technique technique consists in driving the RCM on selected spatial scales only and does not affect the small scales fields since only the large scales are relaxed [Eq. (2)].

$$\partial_t q_{LB} = F(q_{LB}) - \frac{1}{\tau}\left[q_{LB}^{ls} - q_{DF}\right] \qquad (2)$$

where q_{LB}^{ls} is the large-scale part of the LB simulated field q_{LB}. It is obtained by applying a two-dimensional Fourier filter to q_{LB} (which resolution is that of a typical RCM, i.e. about 50 km resolution) with a cutoff wavelength corresponding to typical GCM resolution (i.e. about 300 km). As for indiscriminate nudging, spectral nudging in WRF can only be applied to the wind components and

Fig. 1 Big-Brother experiment approach using a limited area model (LAM) as a regional climate model (RCM)
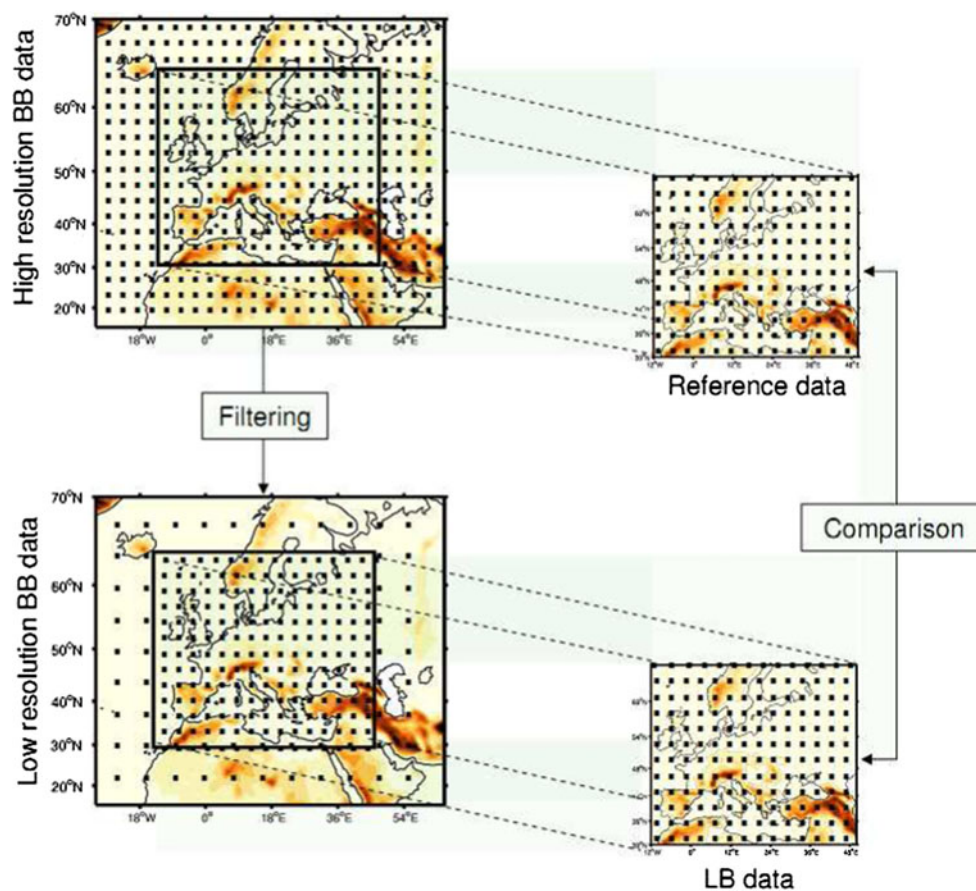
potential temperature. Spectral nudging is applied above the planetary boundary layer with a constant nudging coefficient which is chosen equal for all nudged variables.

2.3 Simulations

An ensemble of 144 simulations has been performed with varying domain size, update frequency of the driving large-scale fields (τ_a) and nudging time (τ) for winter and summer and for indiscriminate and spectral nudging (Table 1). The BB simulation was performed over a large domain covering Europe and North Africa (Fig. 2) with 130×140 horizontal grids points with a 50 km horizontal mesh grid (as required within CORDEX) and 28 vertical levels, the model top is 50 hPa. A winter simulation starts on 1 December 1989–28 February 1990 with 1 month spin up (November 1989) and a summer time simulations from 1 June 1999 to 31 August 1999 with 1 month spin up (May 1999). The initial and boundary conditions of the BB simulation are provided by the ERA-interim reanalysis of the European Center for Medium-range Weather Forecast (ECMWF). The resolution of the BB fields are then degraded using a simple low pass averaging filter to obtain a resolution of 300 km × 300 km (typical GCM resolution) from the 50 km × 50 km fields. It must be noted here

that the nature of the initial and boundary conditions used to drive the BB does not matter as long as they represent a possible realization of the atmospheric state, past or future. The impact of the quality of the driving large-scale fields is out of the scope of this study. The aim of this study is to achieve the best dynamical consistency between the driving large-scale field and the small-scale field simulated with a nudged LAM as a RCM.

In this work it is thus not important whether the model producing the driving fields aims at modelling the actual history of the atmosphere like reanalyses, or aims only at modelling a possible realization of atmospheric dynamics

Table 1 Summary of performed simulations

Domain	Mediterranean	Europe
Resolution (km)	50×50	50×50
Grid dimensions	54×90	98×100
Period	(JJA), (DJF)	(JJA), (DJF)
Analysis frequency τ_a (h)	3, 6, 12	3, 6, 12
Nudging type	NN, IN, SN	NN, IN, SN
Nudging time τ (h)	1, 3, 6, 12	1, 3, 6, 12

The acronyms JJA, DJF, NN, IN and SN stand for June–July–August, December–January–February, no nudging, indiscriminate nudging and spectral nudging, respectively
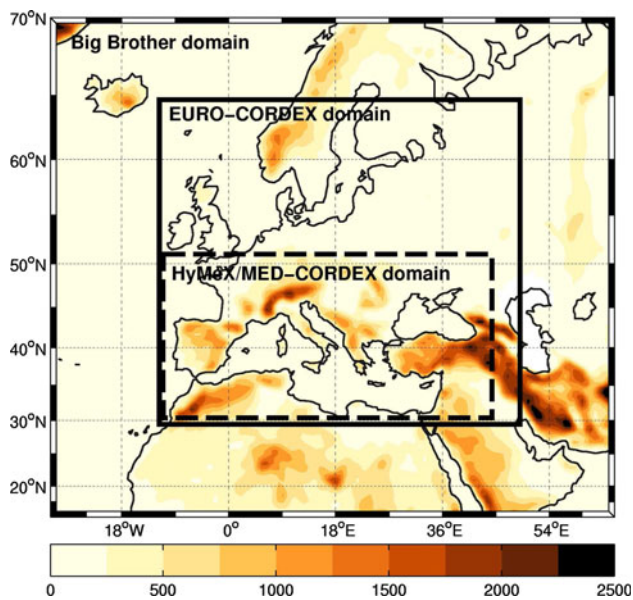
Fig. 2 The Big Brother experiment domains and topography in meters (*color shading*) as represented in WRF. The Europe and Med domains correspond to the EURO–CORDEX and HyMeX/MED–CORDEX domains of the HyMeX and CORDEX international programs

like in climate modelling, be it purely atmospheric or coupled. Therefore in terms of the downscaling typology presented in Castro et al. (2005) our work could be relevant to types 2, 3 or 4 depending on which type of fields are used to drive the regional model. However, renanalyses are an accurate characterization of the global weather, but global climate simulations for both past and future climates are not (e.g. Stephens et al. 2010; Fyfe et al. 2011; Sun and Liang 2012; Xu and Yang 2012; Van Oldenborgh et al. 2012; Van Haren et al. 2012). The proposed strategy ensures a dynamical consistency between the driving field and the simulated small-scale field but it does not ensure the best observed fine scale field because of the possible impact of uncorrect driving large-scale field. This type of downscaling provides an upper bound on the skill possible for recent historical past and twenty-first century projections. Our optimal nudging strategies with respect to dynamic downscaling could add skill whenever the parent global model has some level of skill. For these types of downscaling, as for gobal climate models, post-processing with de-biasing techniques is needed to correct the misrepresented features of the regional climate. This is also absolutely needed for impact studies which are a key objectives of CORDEX.

When nudging (IN and SN) is used, it is applied above the planetary boundary layer as suggested by Lo et al. (2008). The nudged variables are the potential temperature, wind and moisture.

Two CORDEX domains with different domain sizes are used in the model sensitivity experiments. These are the

EURO–CORDEX and HyMeX/MED–CORDEX domains covering Europe and the Mediterranean regions (Fig. 2). The HyMeX/MED–CORDEX domain is embedded within the EURO–CORDEX domain (the HyMeX/MED–COR-DEX domain is smaller since a strong focus is put on ocean/atmosphere coupled runs which requires more computer resources). This "nested" domain approach allows to compare the two sensitivity experiments on the common domain (i.e. the HyMeX/MED–CORDEX domain).

The investigated region is also of strong climate interest since located in a transition zone between the humid western and central European domain and the arid North African desert belt and it is affected by interactions between mid-latitude and tropical processes. It displays a very pronounced seasonal cycle characterized by wet-cold winters and dry-warm summers (Peixoto et al. 1982). Winter in the region is strongly affected by large scales patterns. At the southern limit of the North Atlantic storm tracks, the region is particularly sensitive to interannual displacement of the trajectories of mid-latitude cyclones that can modulate the precipitation (Rodriguez Fonseca and Castro 2002). In the summer, high pressure and descending motions dominate over the region, leading to high temperature and long periods of drought (Xoplaki et al. 2004; Trigo 2006; Stéfanon et al. 2012). In addition to global scale processes and teleconnections, the regional climate is affected by local processes induced by the complex physiography of the region and the presence of the Mediterranean Sea, such as strong regional winds (e.g. Drobinski et al. 2001; Drobinski et al. 2005; Guénard et al. 2005, 2006) and heavy precipitation (e.g. Ducrocq et al. 2008). The contrast between the two seasons prompted us to conduct our studies on two different periods because the physical and dynamical processes involved are not the same and the effect of nudging may differ between winter and summer.

In the following, we identify simulations over the Mediterranean domain as LB–Med and over Europe as LB–Euro. Contrary to Omrani et al. (2012b), we can not use a wide range of values for the update frequency of the driving large-scale fields τ_a because of the diurnal cycle. The value of τ_a is thus always smaller than 12 h.

To quantify the ability of the LB to reproduce the reference field, we used a set of diagnostics similar to those used in Omrani et al. (2012a, b) to facilitate their interpretation. The mean bias δ, the standard deviation σ and the correlation coefficient γ.

3 Results over the EURO–CORDEX domain

In this section we will investigate our results over Europe. In the following, the diagnostics are produced for the surface temperature and wind and for rainfall, for both sake of

simplicity and because they are key variables for climate variability analysis and impact studies. One must note that precipitation is not nudged but produced by the physical parameterizations of the WRF model. Therefore, nudging has an indirect effect on precipitation through temperature, humidity and wind through moisture convergence, for instance. Conversely, even though nudging is not applied within the planetary boundary layer, surface temperature and wind are more directly affected by the nudging term.

3.1 Surface temperature field

Figure 3 shows the Taylor diagram for the total space-time surface temperature in summer (Fig. 3a) and winter (Fig. 3b) for the simulations performed in the absence of nudging (NN with star marker ★) and in the presence of nudging (IN with circle marker ◯ and SN with square marker □). The Taylor diagram provides a way of graphically summarizing how closely a pattern (or a set of patterns) matches reference field (Taylor 2001). The similarity between two patterns is quantified in terms of their correlation (γ) , their centered root-mean-square difference (ϵ) and the amplitude of their variations (represented by their standard deviations σ). Notice that we first substract at each grid point the seasonal mean before computing the

space-time standard deviation and the space-time root-mean-square difference. The LB patterns that agree well with BB are the nearest from the point marked "BB" on the x axis. These patterns have relatively high correlation and low errors. Models lying on the arc corresponding to the standard deviation σ value of the reference have the correct standard deviation (which indicates that the pattern variations are of the right amplitude).

For both seasons, we can only distinguish two ensembles of markers. An ensemble of three points with star marker corresponds to the NN simulations using different update frequencies for the driving large-scale fields ($\tau_a = 1, 3, 6$ and 12 h). These simulations have the lowest correlation coefficients and the highest root means square error compared to the second ensemble which corresponds to the nudged simulations (IN and SN). They have a higher standard deviation compared to the BB in summer and almost the same in winter. This shows that independently of the type or the strength of nudging, IN and SN simulations have the highest skills with respect to the NN simulations. Looking in details, we note that the model skill to reproduce the reference temperature (BB) increases as the updating time (τ_a) decreases. Comparing IN and SN we note that in summer, IN simulation have the highest correlation coefficient, however the SN simulations standard deviation is

Fig. 3 Taylor diagram for surface temperature in summer (**a**) and in winter (**b**) obtained from the LB simulations over the EURO–CORDEX domain. The *red dot* indicate the skill target for the LB simulations ("BB" stands for Big-Brother). The *stars*, *circles* and *squares* display the skill scores of the NN, IN and SN simulations in the Taylor diagram, respectively. The *red*, *blue* and *black colours* correspond to $\tau_a = 3, 6$ and 12 h, respectively. The numbers *1*, *3*, *6* and *12* indicate the values of the nudging time ($\tau = 1, 3, 6$ and 12 h, respectively). Zooms into the *small rectangles* are displayed on the *right panels*
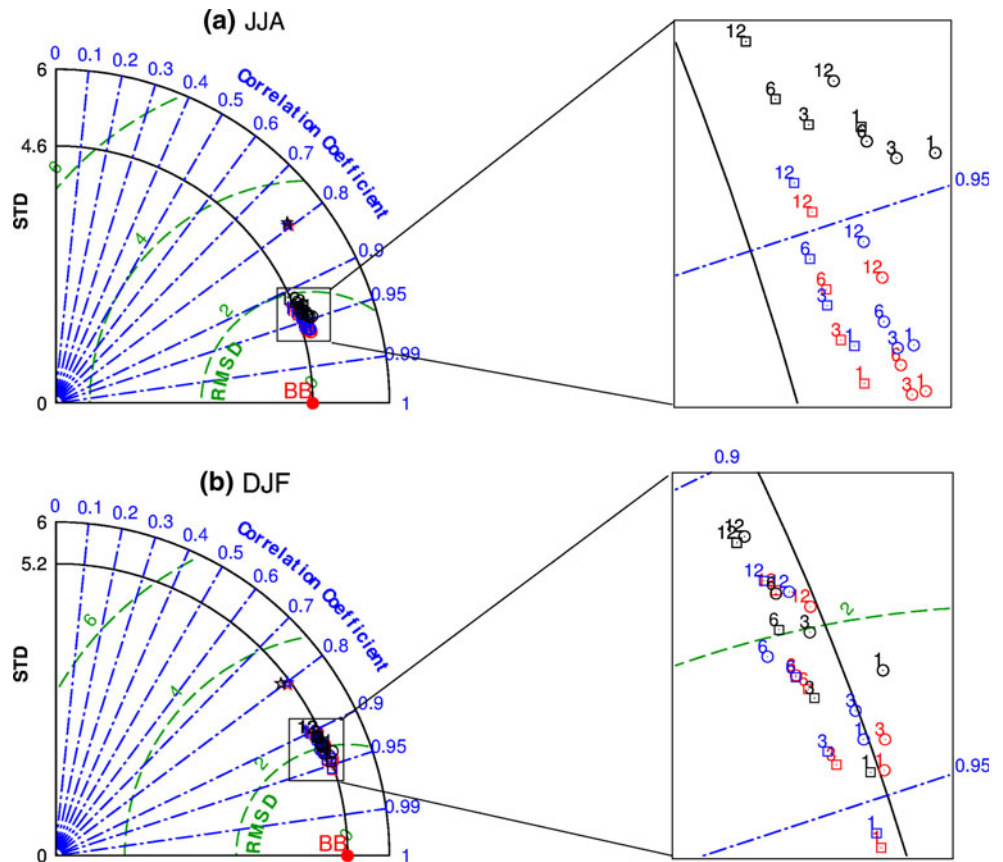
closer to the BB standard deviation value. Nevertheless, the difference between the nudged simulations is very small and thus its significance may be questionable.

The Taylor diagram is a good way to get an overview of the results but it must be accompanied by space-time diagnostics. Figure 4 shows the mean biases between the BB and LB–Euro simulations in the surface temperature in summer and winter for the NN (Fig. 4a, d), IN (Fig. 4b, e) and SN simulations (Fig. 4c, f). In summer, when nudging is not used, we notice a strong warm bias (about +10 °C) over Europe and north Africa mainly over land and the domain centre. This bias is very weak over the sea because the sea surface temperature (SST) is prescribed from ERA-interim reanalysis for all simulations, whereas over land the LSM computes its own surface temperature. In IN and SN simulations, this bias decreases to about ± 2 °C. The difference between the two types of nudging is not significant. Unlike the summer, in winter we note a strong cold bias (about −6 °C) in Eastern Europe and a smaller bias over almost the whole domain in the NN simulation. This bias also disappears in the nudged simulations. The same behavior is found when using larger τ_a values (6, 12 h) (not shown).

This result is consistent with the work of Radu et al. (2008). Comparing non nudged and spectrally nudged simulations performed with the spectral RCM ALADIN over Europe, they found a similar problem of warming over Southeastern Europe related to a dry bias in summer through a positive feedback (Rowell and Jones 2006) and a smaller one in winter. Such summer bias has also been observed in other studies with WRF model (e.g. Caldwell et al. 2009) and explained by an overprediction of daily-maximum temperature which is correlated with a low soil

moisture content. In the present work, the summer bias of the soil moisture is very small (not shown) because we use the 5 layer land-surface model which predicts only soil temperature and prescribes moisture availability given the land surface cover (Bukovsky and Karoly 2009). So these explanation does not hold. Another mechanism must therefore be invoked.

The work by Bowden et al. (2012) also showed a temperature bias over North America when nudging is not used. They showed a significant correlation with a 500 hPa geopotential height bias. Figure 5 shows the 500 hPa geopotential height mean bias between the BB and LB–Euro simulations when nudging is not used (Fig. 5a, d) and for IN (Fig. 5b, e) and SN (Fig. 5c, f) simulations. The 500 hPa geopotential height bias pattern is very similar to that of the temperature (Fig. 4). This result is consistent with the work of Bowden et al. (2012). The increase in temperature corresponds to an atmospheric blocking situation artificially created by the model when nudging is not used. To check whether the blocking is due to dynamical process linked to the synoptic circulation over this region or to numerical deficiencies, the simulation domain has been shifted eastwards (upper row of Fig. 6) and westwards (lower row of Fig. 6) with respect to the reference simulation (middle row of Fig. 6) (the domain size is kept unchanged). This experiment showed that the positive anomaly persists. Its maximum is always located in the center of the domain and extends horizontally over a range roughly corresponding to the domain size. This reveals the numerical nature of this anomaly. This can be easily explained by the feedback of the small scale energetic features produced in the NN simulations towards the larger scales. After some time, the NN

Fig. 4 The mean bias (°C) between the LB simulations with respect to the BB simulation of the surface temperature (i.e. at 2 m height) for summer (**a**, **b**, **c**) and for winter (**d**, **e**, **f**) over the EURO–CORDEX domain. The nudging time τ and update frequency of the large-scale driving fields τ_a are set to 1 and 3 h, respectively. The *left* (**a**, **d**), *middle* (**b**, **e**) and *right* (**c**, **f**) *columns* correspond to the NN, IN and SN simulations, respectively
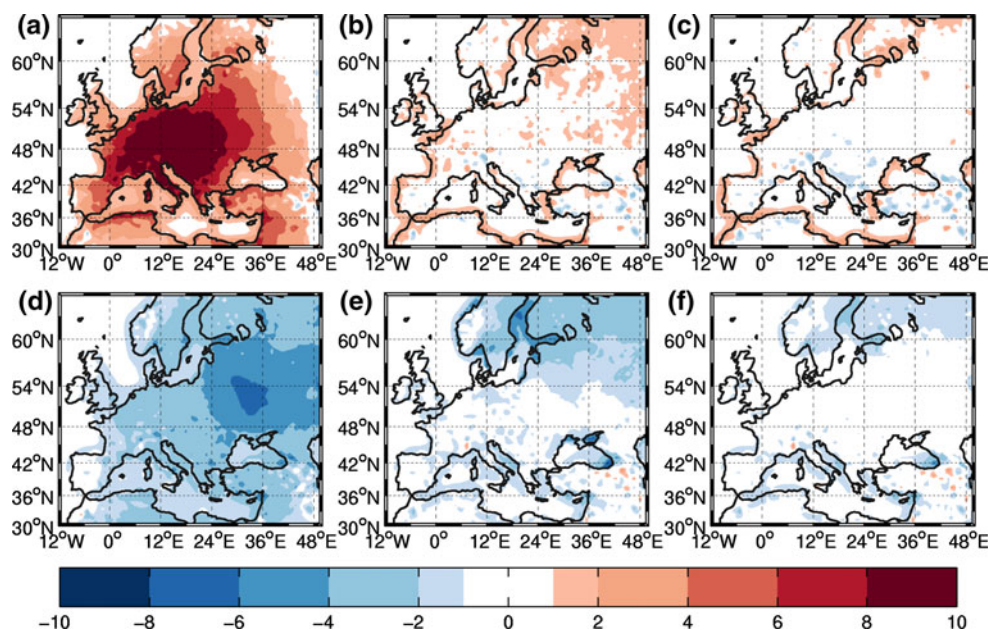
simulations thus produces in the center of the domain a large-scale atmospheric circulation which is "inconsistent" with the large-scale atmospheric circulation imposed at the domain boundaries. The NN simulations finally produces a balanced solution for the large-scale atmospheric circulation different from that of the driving large-scale field within the LB domain.

Figure 7 displays the correlation coefficient γ computed for the surface temperature field as a function of the nudging time τ. It is splitted into the large scale component (γ_{ls}) and the small scale component (γ_{ss}) as in Salameh et al. (2010), Omrani et al. (2012a, b). The surface temperature field is decomposed into a large-scale part and a small-scale part by application of the same low-pass and high-pass 2-D averaging filters used in the BBE with cutoff scale $\Delta = 300$ km. The sum of the large and small scale components is referred as the total surface temperature field (γ_{tot}). The different curves correspond to IN and SN simulations using different values of τ_a. The correlation coefficient is very high for the total and large scale fields (γ_{tot}, $\gamma_{ls} > 0.9$). The correlation γ_{ss} between the BB and LB–Euro small-scale surface temperatures is also fairly high with values ranging between about 0.75 (winter) and 0.80 (summer). The difference between summer and winter is significant since it exceeds the spread of the ensemble of simulations performed for summer on the one hand and for winter on the other hand. This can be explained by the fact that during summer, strong and persistent anticyclonic conditions associated with low cloudiness (and rainfall) make the surface temperature field more predictable. In winter, despite a strong large scale forcing, the temperature field is strongly controlled by cloudiness and precipitation

at small scales which are less predictable variables in numerical modeling. In winter, the difference between IN and SN simulations is not significant. In summer, the IN simulations have systematically higher skill scores than SN simulations. Notice that the increased skill of IN simulations is however not very large (0.82 correlation compared to 0.80 for SN) and possibly sensitive to, e.g. the choice of the cut-off wavenumber for SN. The dominant contribution of the large scales to the total surface temperature field has also been evidenced by Di Luca et al. (2012a) who quantified the added value of the use of RCM at fine horizontal resolution to predict surface temperature and rainfall fields. Looking in detail, Fig. 7 shows that the IN simulations display a peak of maximum correlation for the small-scale component of the surface temperature field. This maximum is found for $\tau = 3$h. The significance of this maximum can be questioned but there is good chance that such maximum exists since expected from the previous studies by Salameh et al. (2010) and Omrani et al. (2012a). Moreover, by applying their theoretical linear prediction to actual numerical simulations with the MM5 model (e.g. Dudhia 1993); Salameh et al. (2010) found an optimum for $\tau = 3.4$ h which is very close to our results. For SN simulations, such a peak is not visible except maybe for the small-scales when $\tau_a = 12$ h (see dashed black curve). This can be due to time-sampling errors as suggested by Omrani et al. (b). Indeed there may be phenomena with a spatial scale larger than $\Delta = 300$ km and a characteristic time scale shorter than 12h. When $\tau_a = 12$ h, such scales are spatially resolved but poorly time-sampled in the forcing fields. These sampling errors can then propagate into the BB model.

Fig. 5 Same as Fig. 4 for geopotential height (m) at 500 hPa
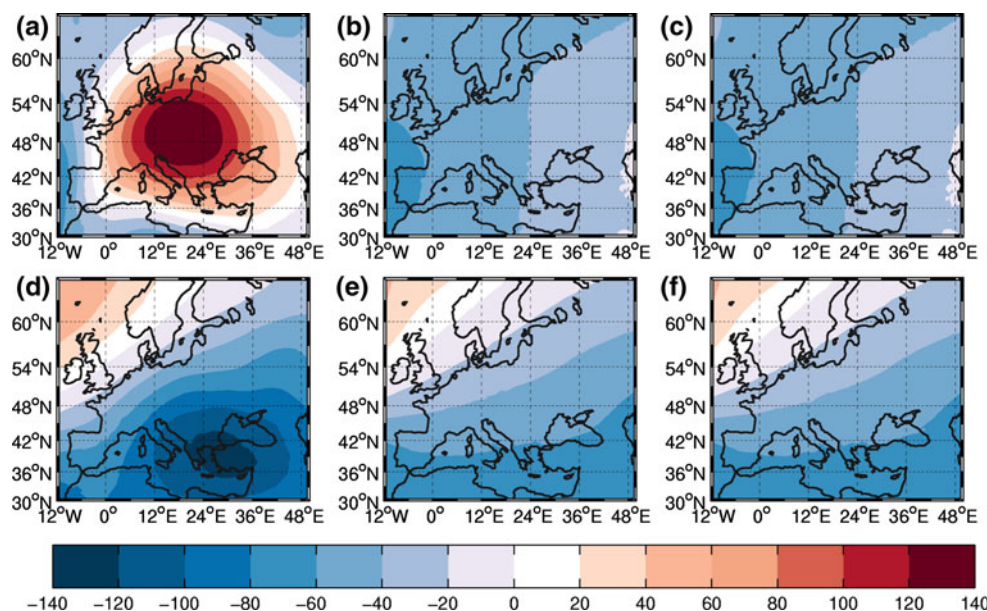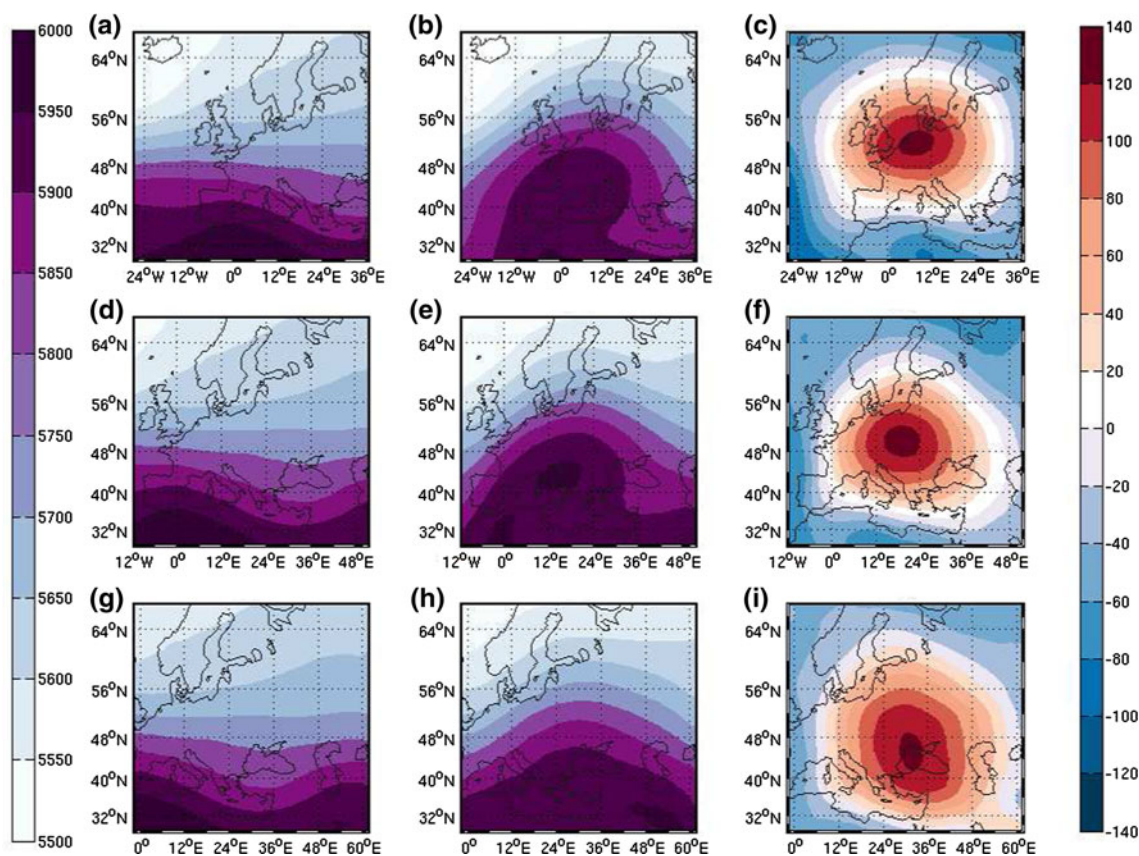
Fig. 6 Five-hundred hPa geopotential height mean (*m*) for the BB (*left colum* **a**, **d**, **g**) and NN simulations (*middle column* **b**, **e**, **h**) and bias (*right column* **c**, **f**, **i**). The *upper row* (**a–c**) correspond to the LB simulation domain shifted westward, the *middle row* (**d–f**) to the reference simulation and the *lower row* (**g–i**) to the LB simulation domain shifted eastward

3.2 Surface wind field

Figure 8 shows the mean bias of the zonal surface wind component (*u* component) for summer and winter from the NN, IN and SN simulations. In summer, the NN simulation displays the largest negative bias over the Mediterranean Sea where it can reach -4 ms^{-1} in some location. It displays the largest positive bias over the Gibraltar Strait where it exceeds 3 ms^{-1}. Slightly lower biases are found over Northwestern Europe (about -3 ms^{-1}) and Central Europe ($+1$–2 ms^{-1}). The IN and SN simulations show no bias over land and the Mediterranean Sea. A residual bias remains over the Atlantic Ocean but its magnitude is significantly reduced (between -1 and -2 ms^{-1}). In winter, the zonal surface wind difference between BB and LB–Euro simulations is negative and can reach values of about -4 ms^{-1}. When nudging is used the bias disappears almost completely over land but a negative bias persists over the sea. The bias is slightly smaller over the Atlantic Ocean near the western boundary of the domain but it increases over the Mediterranean Sea.

Figure 9 is similar to Fig. 8 for the meridional surface wind component (*v* component). We first note that the

spatial pattern of the bias is different from the that of the zonal surface wind component. For both summer and winter, the bias is slightly smaller than for the zonal surface wind component. In summer, the most significant biases are found in the vicinity of the main mountain ranges surrounding the Mediterranean Sea. It is particularly evident in the Northwestern Mediterranean basin over the "Alpine arc" composed of the Pyrennes, Massif Central and the Alps and in North Africa over the Atlas mountain. As for the zonal surface wind component, when nudging is applied (IN and SN simulations), the bias is almost supressed over land, whatever the season. In summer, the residual bias over the Atlantic Ocean is positive contrary to the zonal surface wind component but with nearly the same magnitude (Fig. 8b, c). This advocates for a difference in wind direction and not in wind speed. Even over the Atlantic Ocean, the effect of nudging is thus beneficial. In winter, the use of nudging seems to degrade the surface wind field over the Atlantic Ocean. Indeed, the difference between BB and LB–Euro increases for IN and NN simulations with respect to NN simulations. The difference remains negative as for the zonal surface wind components. The magnitude of the difference is similar for the zonal and
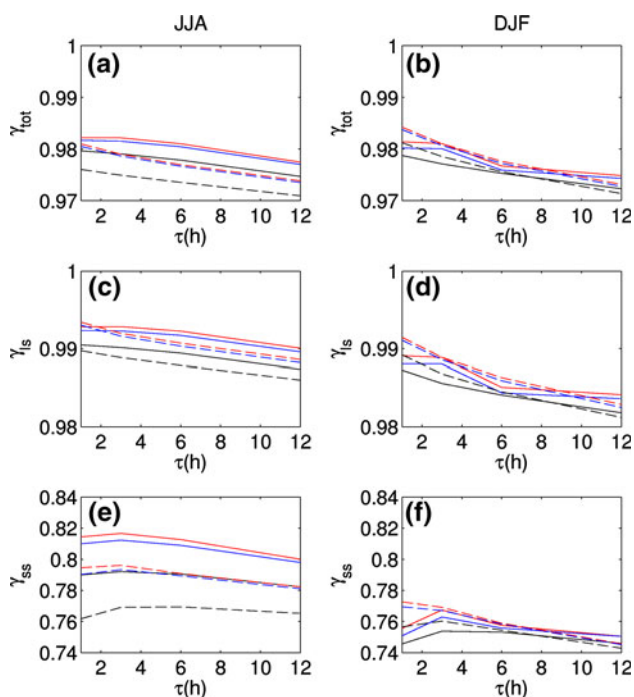
Fig. 7 Correlation coefficient γ between the LB and BB simulations for the surface temperature (i.e. at 2 m height) as a function of the nudging time τ. The results are shown for summer (*left column* **a**, **c**, **e**) and winter (*right column* **b**, **d**, **f**) and for the total field γ_{tot} (*upper row* **a**, **b**), the *large scale* γ_{ls} (i.e. *scales* ≥ 300 km) (*middle row* **c**, **d**) and the *small scale* γ_{ss} (*lower row* **e**, **f**) . The *solid and dashed lines* indicate the results from the IN and SN simulations. The *red, blue and black colors* correspond to values of update frequency of the driving large-scale fields $\tau_a = 3, 6$ and 12 h, respectively

meridional wind components implying that nudging affects here the wind speed and not the wind direction. The reason for such different behavior in summer and winter is still to be understood. Finally, one can note that there is no

sensitivity to the type of nudging used to relax the LB-Euro simulations towards the driving large-scale fields.

Figure 10 displays the correlation coefficient as a function of the nudging time for the surface wind speed at 10 m height. Even smaller than for the surface temperature, the correlation coefficient is also high. For the total and the large scale parts, the correlation coefficients γ_{tot} and γ_{ls} are high (>0.85), because the relaxation is strong enough to prevent LB–Euro field to depart from the driving fields. The small scale part is less accurately simulated. The correlation coefficient γ_{ss} can reach a fairly good value of 0.65 but can be as low as 0.45. Indeed, for both IN and SN simulations, we obtain a bell shape curve for γ_{ss} as a function of τ with a maximum between 0.5 and 0.6 for τ = 3 h. As for the surface temperature, the reason for the similarity of the bell shape curve for γ_{ss} for the IN and SN simulations differs for the two nudging techniques. In the IN simulations and for τ = 1 h, the production of small scales is inhibited because the LB fields are too tightly constrained by nudging to the large-scale driving fields. As the nudging time increases (τ > 1 h), the correlation coefficient reaches a maximum around τ = 3 h and then decreases for large τ values (Omrani et al. 2012a). In the SN simulations, the nudging does not affect the small scales but for example for $\tau_a = 12$ h, the smallest scales present in the large scale driving fields are probably not well resolved in time (Omrani et al. 2012b). However, a still open question is why γ_{ss} displays a bell-shape curve for $\tau_a = 3$ and 6 h while it only occurs for $\tau_a = 12$ h when surface temperature is considered (Fig. 7). Finally, one can note that the correlation coefficient γ_{ss} decreases when τ_a increases for both IN and SN simulations. Indeed for $\tau_a = 12$ h, too few information are provided as boundary conditions. The interpolation between two consecutive large-

Fig. 8 Same as Fig. 4 for the zonal surface (i.e. at 10 m height) wind component u (ms^{-1})
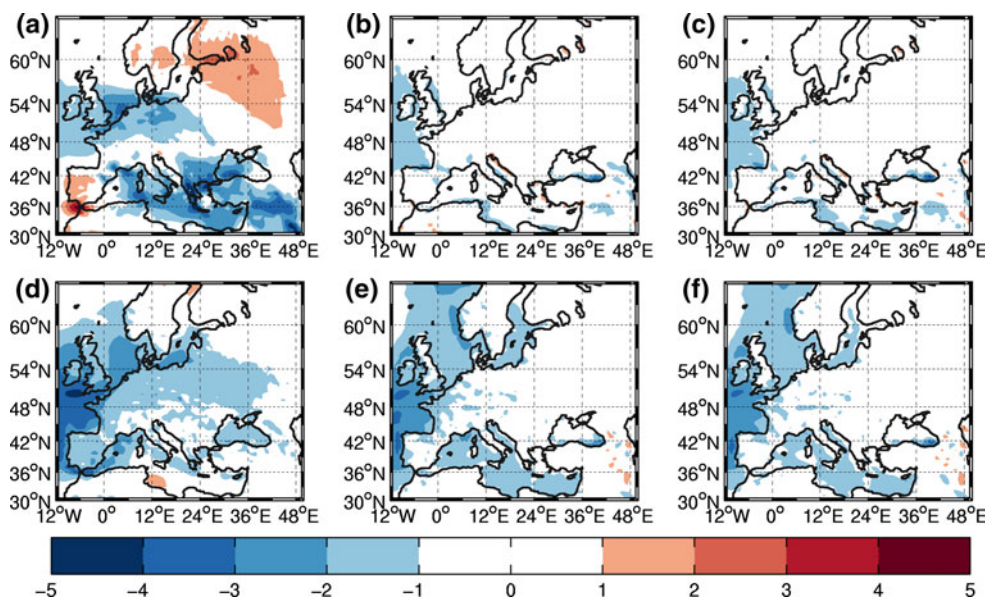
Fig. 9 Same as Fig. 4 for the meridional surface (i.e. at 10 m height) wind component v (ms^{-1})
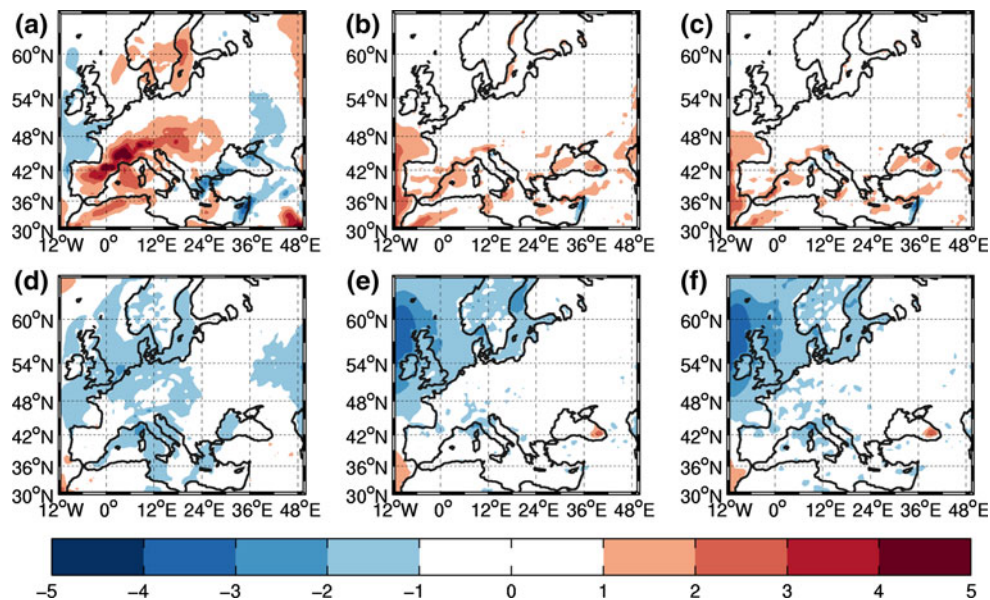
scale driving fields also degrades the dynamics of the atmospheric circulation at the domain boundaries so that the correlation coefficient for both the large-scale part (γ_{ls}) and the small-scale part (γ_{ss}) decreases.

3.3 Precipitation field

Figure 11 displays the Taylor diagram for the total space-time summer and winter precipitation computed from the
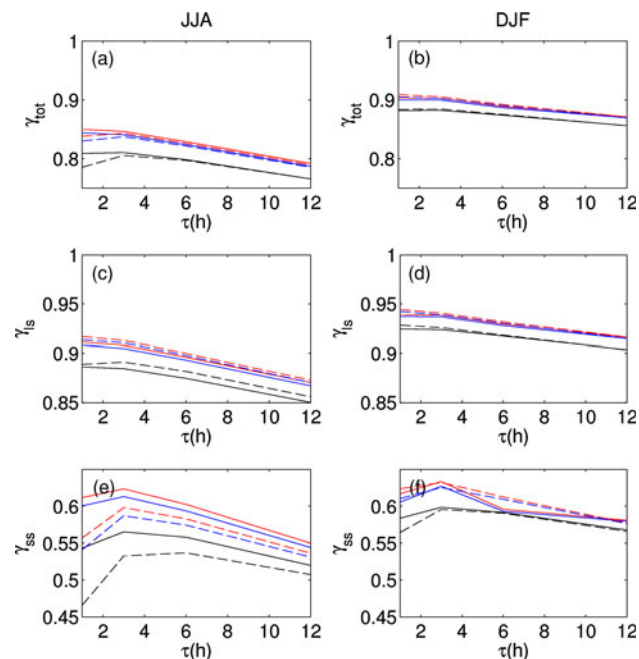

Fig. 10 Same as Fig. 7 for the surface wind speed (i.e. at 10 m height)

NN, IN and SN simulations for different nudging time (τ) and update frequency of large-scale driving fields (τ_a). Again we first substract at each grid point the seasonal mean before computing the space-time standard deviation and the space-time root-mean-square difference. We note that for NN simulations, the precipitation field is poorly correlated to the BB fields compared to IN and SN simulations. SN simulations produce the highest skill score for the smallest nudging time ($\tau = 1$ h) with respect to the other SN simulations. The correlation coefficient γ is >0.4 in summer and >0.6 in winter. However, IN simulation gives the highest scores among all performed simulations for $\tau = 3$ h as also found in Salameh et al. (2010). We also note that in summer, the SN simulations have systematically a higher standard deviation compared to BB, however the IN simulations display a smaller standard deviation for all updating and nudging times (τ_a, τ). In winter, all the simulations have a smaller standard deviation with respect to BB.

Figure 12 displays the summer and winter precipitation bias for NN, IN and SN simulations with $\tau = 1$ h and $\tau_a = 3$ h. In summer and for NN simulation, we note a dry bias (about 2 mm day^{-1}) over a large area of Eastern Europe. This may be partly explained by the positive anomaly of the 500-hPa geopotential height in summer (Fig. 5a), which induces a well-know soil moisture/precipitation feedback (Zampieri et al. 2009; Hohenegger et al. 2009). Indeed, in the absence of nudging, the artificial high pressure over the center of the domain reduces cloud cover and precipitation producing a negative soil-moisture anomaly (not shown). The lower soil moisture content induces smaller evaporation and higher sensible heat which in turn warms the planetary boundary layer and increases
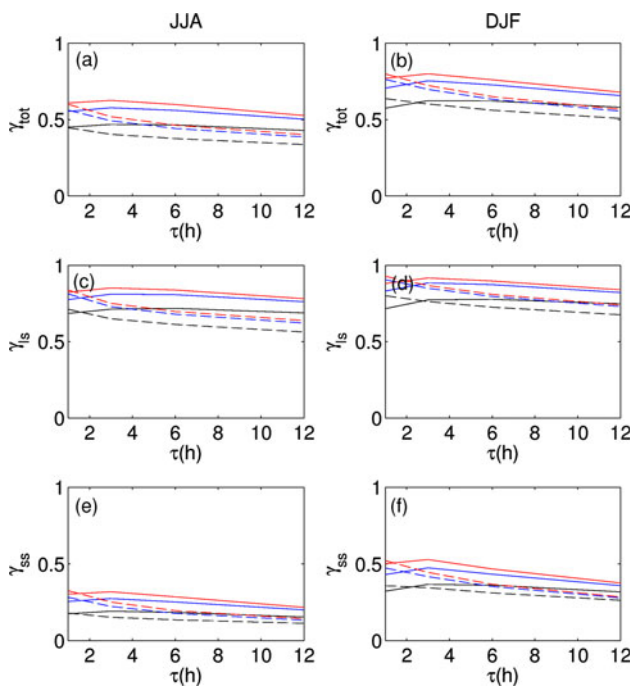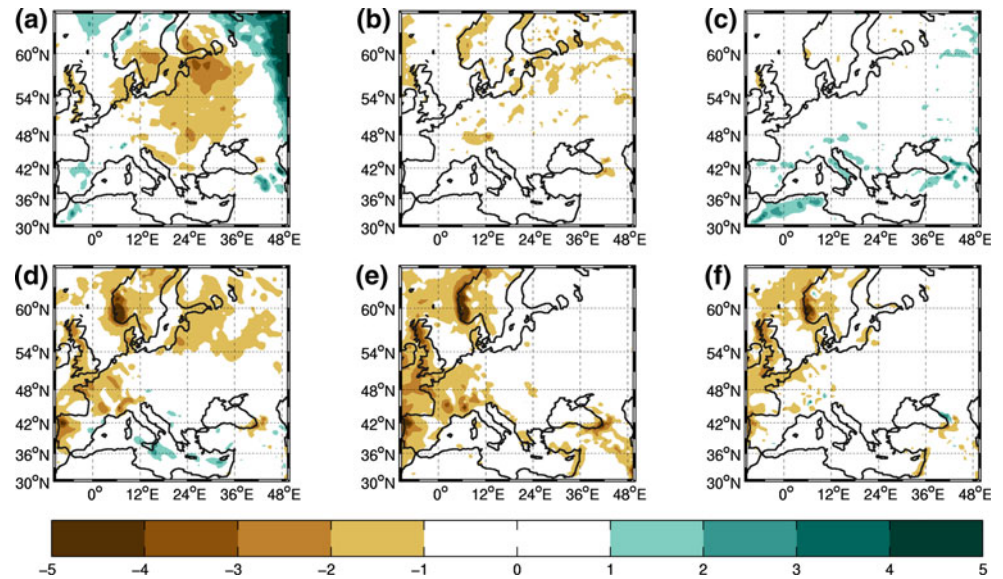
Fig. 11 Same as Fig. 3 for precipitation
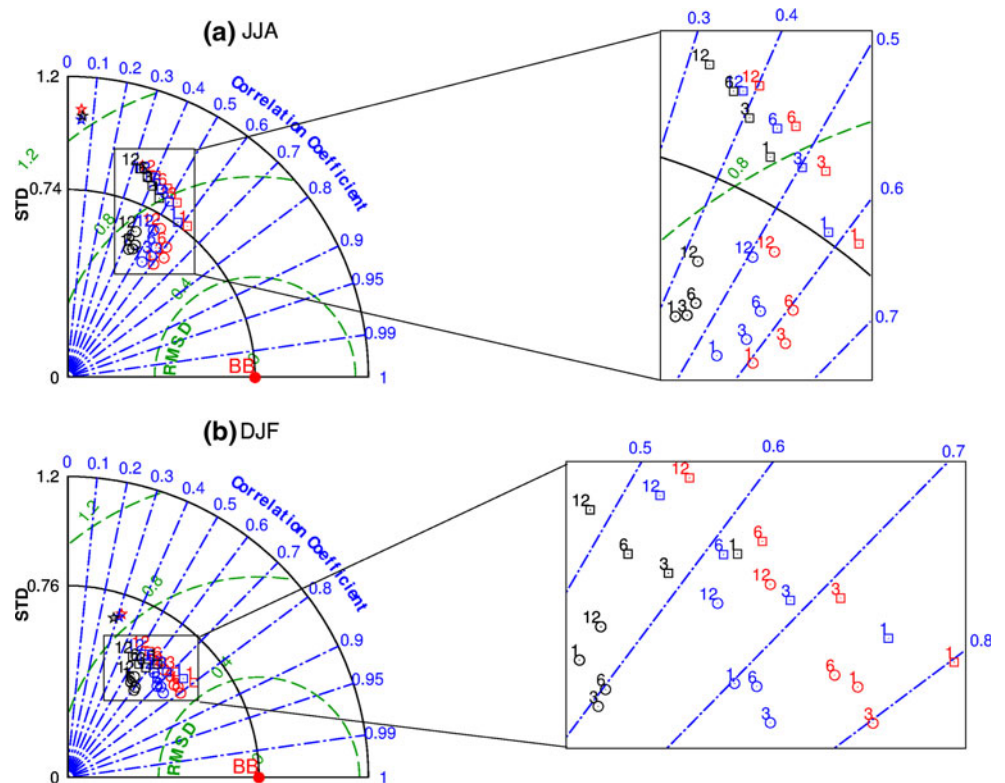
the surface temperature (Fig. 4a). We also note a strong wet bias over the Northeastern boundary of the domain due to the resolution discontinuity between the driving large-scale fields at the domain boundaries and the fine resolution simulated field within the domain. This effect is called the Gibbs effect and is partially smoothed by applying a damping Davies zone. However, some discontinuity is unavoidable which produces strong horizontal gradient of the horizontal wind. The continuity equation imposes the production of strong vertical velocity which can trigger unrealistic precipitation near the domain boundaries. In the following, we remove the data within the Davies zone over the 5 nearest grid points from the domain boundaries. However, when nudging is applied, this effect disappears almost completely. We still have a small dry bias (<1 mm day $^{-1}$) over the whole domain in the IN simulations. Conversely, the SN simulations display a small residual wet bias. Indiscriminate and spectral nudging improve the simulation precipitation but in different ways. In winter, we note a dry bias over the Northern and Western parts of the domain and a small wet bias over the Mediterranean sea in the NN simulation. When nudging is used, precipitation is underestimated over the whole domain, but with a larger magnitude over the Western part of the domain. Spectral nudging seems to have a stronger impact to reduce the bias than IN.

Figure 13 displays the correlation coefficient γ for precipitation in summer and winter for the total field (γ_{tot}),

the large scale part (γ_{ls}) and the small scale part (γ_{ss}). The correlation coefficient for the total field γ_{tot} is larger in winter (0.65) than in summer (0.50) even though we have almost the same scores for the large scale part γ_{ls} (around 0.80). The IN and SN simulations appear to better simulate the small scales in winter than in summer. Indeed, in winter, precipitation comes mainly from the large-scale circulation. Even if the small scale precipitation is not well simulated, the impact on the total field remains marginal. In summer, we have more small-scale precipitations which explains the lower scores of the total field, even though the large scales are correctly simulated . The simulated precipitation display a much weaker sensitivity to the nudging time than surface temperature and wind. The bell-shape curve still exists when IN is used and the optimal nudging time τ is still 3 h, whereas the bell-shape curve is no longer visible when spectral nudging is used. This difference can be explained by the different time scales involved in the dynamics of the temperature, wind and precipitation fields and advocates for possible different optimal nudging time regarding the various variables. Finally, similarly to surface temperature and wind, the correlation coefficient γ decreases when τ_a increases.

Spectral analysis (not shown) shows that, for precipitation, all the scales are overestimated by NN simulations. Conversely, IN simulations underestimate the variance of the small scales which can be expected since all scales are nudged. The SN simulations also tend to underestimate the

Fig. 12 Same as Fig. 4 for precipitation (mm day^{-1})

Fig. 13 Same as Fig. 7 for precipitation

variance of the small scales with however a better agreement with the BB simulations. The sensitivity of the simulated small scale precipitation in IN and SN simulations is larger than the sensitivity of the simulated small scale temperature. It is consistent with Di Luca et al. (2012a, b) who suggest that the potential added value in precipitation simulated by high resolution nested RCMs is higher than for temperature due to the dominant contribution of the large scales for temperature and the dominant contribution of the small scales for precipitation.

4 Comparison with the results over the HyMeX/MED–CORDEX domain

The HyMeX/MED–CORDEX domain being smaller than the EURO–CORDEX domain, the impact of nudging should be damped (Miguez-Macho et al. 2004; Leduc and Laprise 2009; Omrani et al. 2012a). Comparisons of LB–Med simulations with the results obtained over the EURO–CORDEX domain (LB–Euro simulations) are made on the overlapping domain (i.e. the HyMeX/MED–CORDEX).

Figure 14 shows the temperature bias for summer and winter time from the LB–Med and LB–Euro simulations displayed over on the HyMeX/MED–CORDEX domain. Comparing the NN simulations (Fig. 14; left column), we first note that the temperature bias is much stronger in LB-Euro simulations (Fig. 14d, j) than in LB–Med simulations (Fig. 14a, g) for both summer and winter. This confirms the results by Leduc and Laprise (2009) who show that the spatial correlation of the small scale patterns improve when the domain size is reduced. The same effect was observed in a QG model (Omrani et al. 2012a) when it was attributed to the decrease of predictability when the domain size increases. One can also note that the spatial pattern of the surface temperature bias is not the same between NN simulations over the HyMeX/MED–CORDEX and EURO–CORDEX domains. This is due to the location of the LB domains. The center of the LB–Euro simulation domain is located over Central Europe whereas it is located over the Mediterranean Sea for the LB–Med simulations. This produces an anomaly of the 500-hPa geopotential height located in the center of the domains. In summer, the artificial pressure high induces the positive feedback between cloudiness, precipitation, soil moisture and temperature discussed previously. In the LB–Med simulations, the

temperature anomaly is also in part damped by the fact that over the Mediterranean Sea, the effect on the surface temperature is much smaller. In winter, the artificially produced pressure low produces a negative bias of temperature. The interpretation is less straightforward than during summer since the European continent is less locally forced and is under the influence of synoptic disturbances advected form the Atlantic Ocean. However, nudging inhibits the impact of the domain size on the simulated surface temperature whatever the season. This is consistent with the work of Alexandru et al. (2009) and Weisse and Feser (2003) who showed the ability of spectral nudging to reduce the internal variability of the regional model for smaller domain. The comparison between the nudged simulations (IN and SN simulations) does not show significant difference.

Figure 15 shows the Taylor diagram of the surface temperature from the LB–Med and LB–Euro simulations. The difference between the results obtained in the absence of nudging and when nudging is applied (indiscriminate and spectral) is stronger for LB–Euro simulations than for LB–Med simulations, whatever the diagnostic used to evaluate the LB simulations.

Table 2 finally summarizes for all the diagnosed variables, the spatial correlation γ between LB–Euro/LB–Med simulations and the BB simulation over the Mediterreanean domain. For the NN simulations, we see that for all variables and for both seasons, the Mediterranean domain has a higher correaltion than Europe. However, when nudging is used, the correlation coefficients are the same or very close. This confirms the two previous results: nudging reduces the sensitivity of the model to the domain size and the control by the boundaries is significantly more important over the LB–MED simulations even though the LB–Med simulations still need to be nudged.

5 Conclusions and perspectives

In this work, we have analyzed the impact, as a function of the nudging time, of indiscriminate and spectral nudging on an ensemble of simulations performed with the WRF
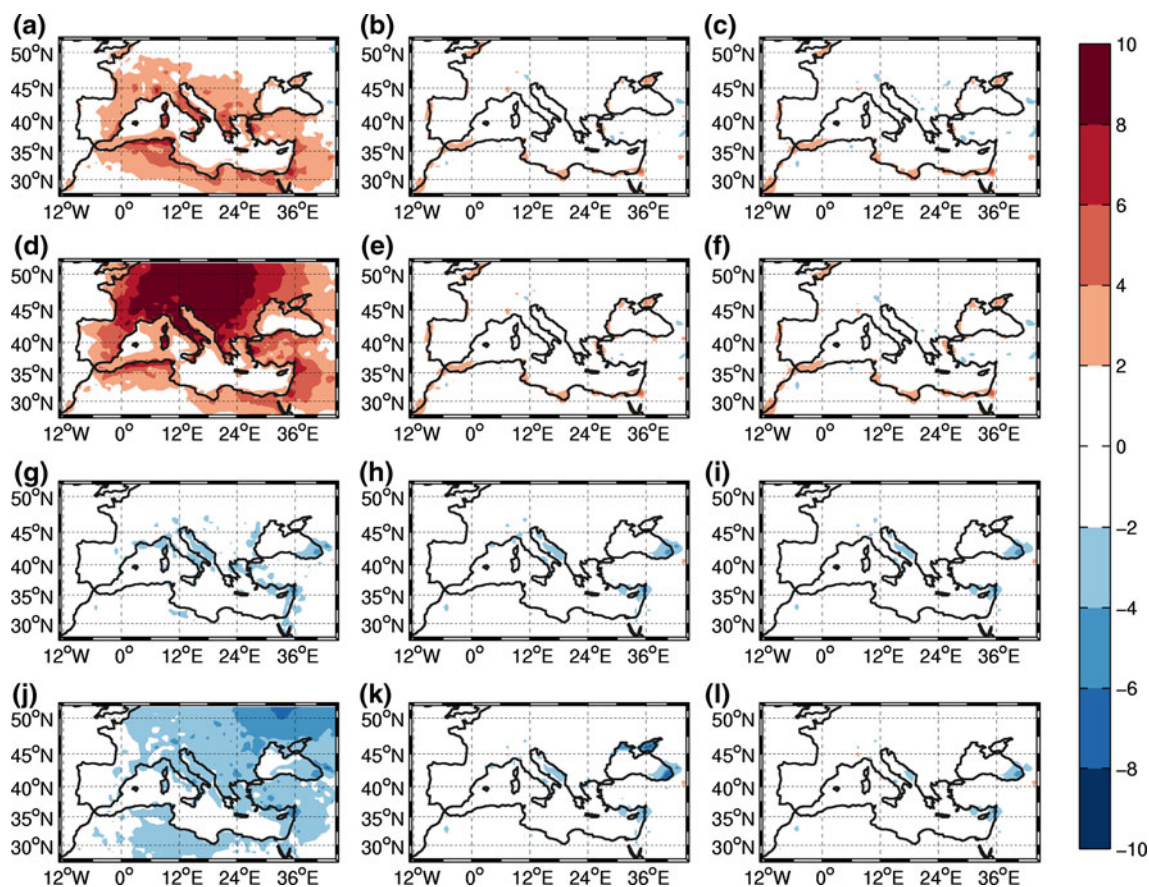
Fig. 14 The mean bias (°C) between the LB simulations with respect to the BB simulation of the surface temperature (i.e. at 2 m height) for summer (*two upper rows* **a–f**) and for winter (*two lower rows* **g–l**) over the HyMeX/MED–CORDEX domain (**a–c** and **g–i**) and EURO–CORDEX domain (**d–f** and **j–l**). The nudging time τ and update frequency of the *large-scale* driving fields τ_a are set to 3 and 1 h, respectively. The *left* (**a, d, g, j**), *middle* (**b, e, h, k**) and *right* (**c, f, i, l**) *columns* correspond to the NN, IN and SN simulations, respectively

Fig. 15 Taylor diagram for surface temperature (i.e. at 2 m height) obtained from the LB simulations over the EURO–CORDEX domain (**a**) and HyMeX/MED–CORDEX domain (**b**). The *red dot* indicate the skill target for the LB simulations ("BB" stands for Big-Brother). The *stars, circles* and *squares* display the skill scores of the NN, IN and SN simulations in the Taylor diagram, respectively. The *red, blue* and *black colours* correspond to τ_a = 3, 6 and 12, respectivel. The numbers *1, 3, 6* and *12* indicate the values of the nudging time (τ = 1, 3, 6 and 12, respectively. Zooms into the *small rectangles* are displayed on the *right panels*
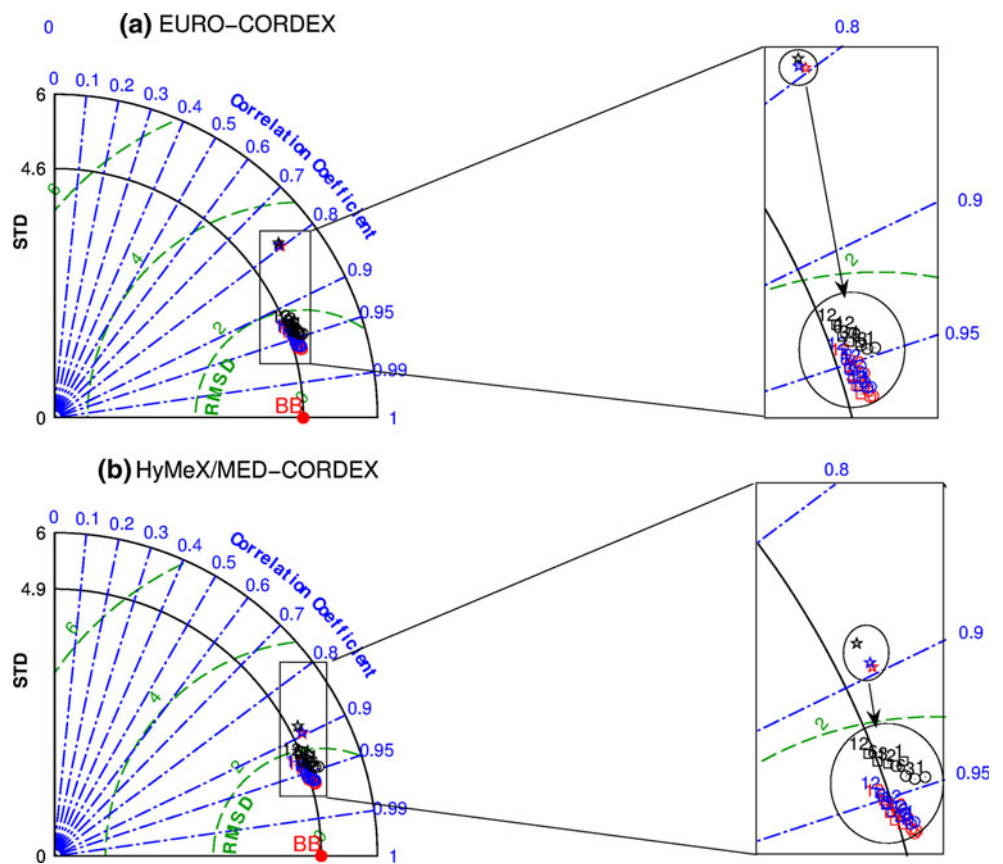
Table 2 Spatial correlation coefficients γ between the LB–Med/LB–Euro and BB simulations computed over the overlapping domain (i.e. the HyMeX/MED–CORDEX domain) for τ = 1 h and τ_a = 3 h

Season	DJF						JJA					
Nudging	NN		IN		SN		NN		IN		SN	
Domain	Euro	Med	Euro	Med	Euro	Med	Euro	Med	Euro	Med	Euro	Med
Surface temperature	0.90	0.94	0.97	0.97	0.97	0.97	0.69	0.89	0.97	0.97	0.96	0.96
Precipitation	0.28	0.36	0.69	0.69	0.74	0.74	0.05	0.16	0.49	0.48	0.45	0.45
Surface zonal wind component	0.66	0.75	0.93	0.93	0.93	0.93	0.38	0.58	0.92	0.91	0.91	0.90
Surface meridional wind component	0.66	0.75	0.93	0.93	0.93	0.93	0.38	0.59	0.91	0.89	0.89	0.87

The acronyms JJA, DJF, NN, IN and SN stand for June–July–August, December–January–February, no nudging, indiscriminate nudging and spectral nudging, respectively

model. We use a BBE framework which eliminates a number of possible sources of errors and allows a comparison all other things being equal. Using this framework we have furthermore addressed the existence of an optimal nudging time maximizing the resemblance of the downscaled fields with reference fields, and we have compared the ability of indiscriminate and spectral nudging to reconstruct the reference fields. This provides an objective and physically based strategy to have the best dynamical consistency between the driving large-scale field and the simulated small-scale field. The optimal time is identified simply by exploring a plausible range of nudging times and

not by a systematic optimization procedure (e.g. Vidard et al. 2003). The ensemble of numerical simulations was performed on two different but overlapping domains to investigate the impact of the size of the domain on the sensitivity to nudging time. Such work was in part motivated by the international downscaling experiment CORDEX. The largest domain is the EURO–CORDEX domain and the smallest domain is the HyMeX/MED–CORDEX domain "nested" in the largest domain. Sensitivity to nudging time is also impacted by the update frequency of driving fields and depends on the variable under consideration. Domain size and update frequency of the large-

scale driving fields are the key parameters identified by Omrani et al. (2012a, b) controlling how the quality of nudged simulations depends on the nudging time. Instead of a nested QG model, we use here a numerical model approaching much better the full complexity of the atmospheric processes. Due to the different nature of the regional Euro-Mediterranean climate in summer and winter, the results have been analyzed for the two seasons separately.

Compared to non nudged configuration, results show that nudging clearly improves the model capacity to reproduce the reference fields from the BB simulations, regardless the domain size and the diagnosed variable. However the skill scores depend on the variable, the season and the update frequency of the driving large-scale fields. When comparing the simulations over the EURO–CORDEX and HyMeX/MED–CORDEX domains, we found that for large simulation domain, the effect of nudging is very positive on the simulated field whereas its effect becomes marginal for small simulation domain because of a strong control by the lateral boundaries. When nudging is applied, the simulations also become insensitive to the domain size. Despite the weaker effect of nudging on the simulations performed over the HyMeX/MED–CORDEX domain, nudging is still needed to improve significantly the simulated regional climate.

The differences between the simulations performed with IN and spectral nudging are not significant. The reasons for which one simulation performed better than the other and vice-versa are not straightforward and no clear behaviour is found. The difference between indiscriminate and spectral nudging that is observed in practice in our RCM runs is much smaller than what one could anticipate based on previous idealized studies (Omrani et al. 2012a, b). We suggest that a reason for this very similar performance is that nudging is active only above the planetary boundary layer, following Lo et al. (2008). Although there is some small-scale activity in the free troposphere, we expect it to be less energetic than in the planetary boundary layer which is forced by surface fluxes and orography. Therefore the detrimental effect of IN on small scales remains limited in practice. IN then has an impact similar to that of spectral nudging. Confirming this suggestion would probably need a dedicated study with a less complex model such as the QG model used in Omrani et al. (2012a, b). Regarding the determination of a possible optimal nudging time, the conclusion is not the same for indiscriminate nudging and spectral nudging and depends on the update frequency of the driving large-scale fields τ_a. For indiscriminate nudging, the optimal nudging time is around $\tau = 3$ h for almost all cases. This value is very similar to Salameh et al. (2010). For spectral nudging, the optimal nudging time τ varies between 1 and 3 h. Indeed, for $\tau_a = 3$ and 6 h, the

highest model skills are found for $\tau = 1$ h. One must note here that $\tau = 1$ h is the smallest value used for the simulations. The optimal nudging time could thus be smaller than 1 h but this has not been investigated, in part due to numerical instabilities produced for very small values of τ. For $\tau_a = 12$ h, the optimum nudging time τ is around 3 h. This can be due to time-sampling errors as suggested by Omrani et al. (b). Indeed there may be phenomena with a spatial scale larger than $\Delta = 300$ km and a characteristic time scale shorter than 12 h. When $\tau_a = 12$ h, such scales are spatially resolved but poorly time-sampled in the forcing fields. These sampling errors can then propagate into the BB model. This is at least true for surface temperature and wind. Such behavior is not evidenced for precipitation. This difference can be explained by the different time scales involved in the dynamics of the temperature, wind and precipitation fields and advocates for possible different optimal nudging time regarding the various variables. Also, in our simulations, all possible variables of WRF have been nudged (temperature, wind and humidity). In the future, the choice of the variables to be nudged will be addressed.

In the context of spectral nudging, it would be interesting to address the impact of the cut-off wavenumber on the sensitivity to nudging time. Recent work by Liu et al. (2012) compares spectrally nudged simulations with different cut-off wavenumbers to NCEP reanalyses. However a single nudging time of 1 h is used. This value is low compared to the optimal value found in the present study and could be unfair to IN. It would be interesting to vary systematically the nudging time and to evaluate the nudged simulations in a BBE framework.

Finally, in real regional climate modeling, the GCM used to drive the RCM have generally different numerical schemes and physical parameterizations (e.g. Kanamaru and Kanamitsu 2007; Thatcher and McGregor 2009). They are a source of enhanced internal variability. In addition, the validation of regional climate simulations must eventually be done by comparing to observations, often using gridded dataset like CRU and ECA&D which have their own uncertainties and biases (Flaounas et al. 2012c). For all these reasons, it must be clear that the ideal optimal nudging configuration of WRF discussed in this study may not at the end produce the best results due to other uncertainty sources.

References

Alexandru A, de Elia R, Laprise R, Separovic L, Biner S (2009) Sensitivity study of regional climate model simulations to large-scale nudging parameters. Mon Weather Rev 137:1666–1686

Bhaskaran B, Jones RG, Murphy JM, Noguer M (1996) Simulations of the Indian summer monsoon using a nested regional climate model: domain size experiments. Clim Dyn 12:573–587

Bowden J, Otte T, Nolte C, Otte M (2012) Examining interior grid nudging techniques using two-way nesting in the WRF model for regional climate modeling. J Clim 25:2805–2823

Bukovsky MS, Karoly DJ (2009) Precipitation simulations using wrf as a nested regional climate model. J Appl Meteorol Climatol 48:2152–2159

Caldwell P, Chin HNS, Bader DC, Bala G (2009) Evaluation of a WRF dynamical downscaling simulation over California. Clim Change 95:499–521

Castro C, Pielke Sr R, Leoncini G (2005) Dynamical downscaling: assessment of value retained and added using the regional atmospheric modeling system (RAMS). J Geophys Res 110: D05108. doi:10.1029/2004JD004721

Claud C, Alhammoud B, Funatsu BM, Lebeaupin-Brossier C, Chaboureau JP, Béranger K, Drobinski P (2012) A high resolution climatology of precipitation and deep convection over the mediterranean region from operational satellite microwave data: development and application to the evaluation of model uncertainties. Nat Hazards Earth Syst Sci 12: 785–798

Crétat J, Pohl B, Richard Y, Drobinski P (2012) Uncertainties in simulating regional climate of southern africa: sensitivity to physical parameterizations using WRF. Clim Dyn 38:613–634

Davies HC, Turner RE (1977) Updating prediction models by dynamical relaxation: an examination of the technique. Q J R Meteorol Soc 103:225–245

De Elia R, Laprise R, Denis B (2002) Forecasting skill limits of nested, limited-area models: a perfect-model approach. Mon Weather Rev 130:2006–2023

Denis B, Laprise R, Caya D, Côté J (2002) Downscaling ability of one-way nested regional climate models: the Big-Brother experiment. Clim Dyn 18:627–646

Denis B, Laprise R, Caya D (2003) Sensitivity of a regional climate model to the resolution of the lateral boundary conditions. Clim Dyn 20:107–126

Déqué M, Piedelievre J (1995) High-resolution climate simulation over Europe. Clim Dyn 11:321–339

Di Luca A, de Elía R, Laprise R (2012a) Potential for added value in temperature simulated by high-resolution nested RCMs in present climate and in the climate change signal. Clim Dyn 1–22. doi:10.1007/s00382-012-1384-2

Di Luca A, de Elia R, Laprise R (2012b) Potential for added value in precipitation simulated by high resolution nested regional climate models and observations. Clim Dyn 38:1229–1247

Drobinski P, Flamant C, Dusek J, Flamant P, Pelon J (2001) Observational evidence and modeling of an internal hydraulic jump at the atmospheric boundary layer top during a tramontane event. Boundary Layer Meteorol 98:497–515

Drobinski P, Bastin S, Guénard V, Caccia J, Dabas A, Delville P, Protat A, Reitebuch O, Werner C (2005) Summer mistral at the exit of the Rhône valley. Q J R Meteorol Soc 131:353–375

Drobinski P, Béranger K, Ducrocq V, Allen J, Chronis G, Font J, Madec G, Papathanassiou E, Pinardi N, Sammari C, Taupier-Letage I (2009a) The HYMEX (hydrological in the mediterranean experiment) program: the specific context of oceanography. Mercator Newslett 32:3–4

Drobinski P, Ducrocq V, Lionello P, The HyMeX ISSC (2009b) Hymex, a potential new CEOP RHP in the mediterranean basin. GEWEX Newslett 19:5–6

Drobinski P, Ducrocq V, Lionello P (2010) Studying the hydrological cycle in the mediterranean. EOS Trans Am Geophys Union 91:373

Drobinski P, Ducrocq V, Lionello P, Homar V (2011) Hymex, the newest GEWEX regional hydroclimate project. GEWEX Newslett 21:10–11

Drobinski P, Anav A, Lebeaupin-Brossier C, Samson G, Stéfanon M, Bastin S, Baklouti M, Béranger K, Beuvier J, Bourdallé-Badie R, Coquart L, D'Andrea F, De Noblet-Ducoudré N, Diaz F, Dutay JC, Ethe C, Foujols MA, Khvorostyanov D, Madec G, Mancip M, Masson S, Menut L, Palmieri J, Polcher J, Turquety S, Valcke S, Viovy N (2012) Modelling the regional coupled earth system MORCE: application to process and climate studies in vulnerable regions. Env Model Softw 35:1–18

Ducrocq V, Nuissier O, Ricard D, Lebeaupin C, Anquetin S (2008) A numerical study of three catastrophic precipitating events over Southern France. II: mesoscale trigerring and stationarity factors. Q J R Meteorol Soc 134:131–145

Dudhia J (1989) Numerical study of convection observed during the winter monsoon experiment using a mesoscale two dimensional model. J Atmos Sci 46:3077–3107

Dudhia J (1993) A nonhydrostatic version of the Penn State/NCAR mesoscale model: validation tests and simulations of an Atlantic cyclone and cold front. Mon Weather Rev 121:1493–1513

Flaounas E, Drobinski P, Vrac M, Bastin S, Lebeaupin-Brossier C, Stéfanon M (2012a) Precipitation and temperature variability and extremes in the mediterranean region: evaluation of dynamical and statistical downscaling methods. Clim Dyn. doi: 10.1007/s00382-012-1558-y

Flaounas E, Drobinski P, Bastin S (2012b) Dynamical dowscaling of IPSL-CM5 CMIP5 historical simulations over the mediterranean: benefits on the representation of regional cyclogenesis. Clim Dyn. doi:10.1007/s00382-012-1606-7

Flaounas E, Drobinski P, Borga M, Calvet JC, Delrieu G, Morin E, Tartari G, R T (2012c) Assessment of gridded observations used for climate model validation in the mediterranean region: the HyMeX and MED–CORDEX framework. Env Res Lett 7. doi: 10.1088/1748-9326/7/2/024017

Fyfe J, Merryfield W, Kharin V, Boer G, Lee W, Von Salzen K (2011) Skillful predictions of decadal trends in global mean surface temperature. Geophys Res Lett 38:L22801. doi: 10.1029/2011GL049508

Giorgi F, Bi X (2000) A study of internal variability of a regional climate model. J Geophys Res 105:29503–29521

Giorgi F, Jones C, Asrar GR (2009) Addressing climate information needs at the regional level: the cordex framework. WMO Bull 58(3):175–183

Guénard V, Drobinski P, Caccia J, Campistron B, Bénech B (2005) An observational study of the mesoscale mistral dynamics. Boundary Layer Meteorol 115:263–288

Guénard V, Drobinski P, Caccia J, Tedeschi G, Currier P (2006) Dynamics of the MAP IOP-15 severe mistral event: observations and high-resolution numerical simulations. Q J R Meteorol Soc 132:757–778

Hewitson BC, Crane RG (1996) Climate downscaling: techniques and application. Clim Res 07:97–110

Hohenegger C, Brockhaus P, Bretherton CS, Schaer C (2009) The soil moisture-precipitation feedback in simulations with explicit and parameterized convection. J Clim 22:5003–5020

Hong SY, Dudhia J, Chen SH (2004) A revised approach to ice microphysical processes for the bulk parameterization of clouds and precipitation. Mon Weather Rev 132:103–120

Hong SYHMHJ, Zhao Q (1998) Implementation of prognostic cloud scheme for a regional spectral model. Mon Weather Rev 126: 2621–2639

Hourdin F, Musat I, Bony S, Braconnot P, Codron F, Dufresne JL, Fairhead L, Filiberti MA, Friedlingstein P, Grandpeix JY, Krinner G, LeVan P, Li Z, Lott F (2006) The LMDZ4 general circulation model: climate performance and sensitivity to parametrized physics with emphasis on tropical convection. Clim Dyn 27:787–813

Kain JS (2004) The Kain Fritsch convective parameterization: an update. J Appl Meteorol 43:170–181

Kanamaru H, Kanamitsu M (2007) Scale-selective bias correction in a downscaling of global analysis using a regional model. Mon Weather Rev 135(2):334–350

Lebeaupin-Brossier C, Drobinski P (2009) Numerical high-resolution air-sea coupling over the gulf of Lions during two tramontane/mistral events. J Geophys Res 114. doi:10.1029/2008JD011,601

Lebeaupin-Brossier C, Béranger K, Deltel C, Drobinski P (2011) The mediterranean response to different space-time resolution atmospheric forcings using perpetual mode sensitivity simulations. Ocean Model 36:1–25

Lebeaupin-Brossier C, Béranger K, Drobinski P (2012a) Sensitivity of the north-western mediterranean coastal and thermohaline circulations as simulated by the 1/12° resolution oceanic model NEMO-MED12 to the space-time resolution of the atmospheric forcing. Ocean Model 43–44:94–107

Lebeaupin-Brossier C, Béranger K, Drobinski P (2012b) Ocean response to strong precipitation events in the gulf of lions (north-western mediterranean sea): a sensitivity study. Ocean Dyn 62:213–226

Lebeaupin Brossier C, Drobinski P, Béranger K, Bastin S, Orain F (2012c) Ocean memory effect on the dynamics of coastal heavy precipitation preceded by a mistral event in the north-western mediterranean. Q J R Meteorol Soc. doi:10.1002/qj.2049

Leduc M, Laprise R (2009) Regional climate model sensitivity to domain size. Clim Dyn 32:833–854

Liu P, Tsimpidi A, Hu Y, Stone B, Russell A, Nenes A (2012) Differences between downscaling with spectral and grid nudging using wrf. Atmos Chem Phys 12:3601–3610

Lo JC, Yang ZL, Pielke RA (2008) Assessment of three dynamical climate downscaling methods using the weather research and forecasting (WRF) model. J Geophys Res 113:D09112

Miguez-Macho G, Stenchikov GL, Robock A (2004) Spectral nudging to eliminate the effects of domain position and geometry in regional climate model simulations. J Geophys Res 109:D13104–D13104

Mlawer EJ, Taubman SJ, Brown PD, Iacono MJ, Clough SA (1997) Radiative transfer for inhomogeneous atmospheres: RRTM, a validated correlated-k model for the longwave. J Geophys Res 102:16663–16682

Noguer M, Jones R, Murphy J (1998) Sources of systematic errors in the climatology of a regional climate model over Europe. Clim Dyn 14:691–712

Noh Y, Cheon WG, Hong SY, Raasch S (2003) Improvement of the k-profile model for the planetary boundary layer based on large eddy simulation data. Boundary Layer Meteorol 107(2):401–427

Omrani H, Drobinski P, Dubos T (2012a) Investigation of indiscriminate nudging and predictability in a nested quasi-geostrophic model. Q J Roy Meteorol Soc 138:158–169

Omrani H, Drobinski P, Dubos T (2012b) Spectral nudging in regional climate modeling: how strongly should we nudge? Q J R Meteorol Soc 138:1808–1813

Peixoto J, deAlmeida M, Rosen RD, Salstein DA (1982) Atmospheric moisture transport and the water balance of the mediterranean sea. Water Resour Res 18:83–90

Radu R, Déqué M, Somot S (2008) Spectral nudging in a spectral regional climate model. Tellus A 60:898–910

Rockel B, Castro C, Pielke Sr R, von Storch H, Leoncini G (2008) Dynamical downscaling: Assessment of model system dependent retained and added variability for two different regional climate models. J Geophys Res 113:D21107. doi:10.1029/2007JD009461

Rodriguez Fonseca B, Castro M (2002) On the connection between winter anomalous precipitation in the Iberian Peninsula and Morocco and the summer subtropical Atlantic SST. Geophys Res Lett 29. doi:10.1029/2001GL014421

Rowell DP, Jones RG (2006) Causes and uncertainty of future summer drying over europe. Clim Dyn 27:281–299

Salameh T, Drobinski P, Dubos T (2010) The effect of indiscriminate nudging time on large and small scales in regional climate modelling: application to the mediterranean basin. Q J R Meteorol Soc 136:170–182

Schraff C (1997) Mesoscale data assimilation and prediction of low stratus in the Alpine region. Meteorol Atmos Phys 64:21–50

Seth A, Giorgi F (1998) The effects of domain choice on summer precipitation simulation and sensitivity in a regional climate model. J Clim 11:2698–2712

Skamarock WC, Klemp JB (2007) A time-split nonhydrostatic atmospheric model for research and NWP applications. J Comput Phys 227:3465–3485

Stauffer DR, Seaman NL (1990) Use of four-dimensional data assimilation in a limited-area mesoscale model. Part I: experiments with synoptic-scale data. Mon Weather Rev 118(6): 1250–1277

Stauffer DR, Seaman NL (1994) Multiscale four-dimensional data assimilation. J Appl Meteorol 33:416–434

Stéfanon M, D'Andrea F, Drobinski P (2012) Heatwave classification over europe and the mediterranean region. Environ Res Lett 7. doi:10.1088/1748-9326/7/1/014023

Stephens G, L'Ecuyer T, Forbes R, Gettlemen A, Golaz J, Bodas-Salcedo A, Suzuki K, Gabriel P, Haynes J (2010) Dreary state of precipitation in global models. J Geophys Res 115:D24211. doi:10.1029/2010JD014532

von Storch H, Langenberg H, Feser F (2000) A spectral nudging technique for dynamical downscaling purposes. Mon Weather Rev 128:3664–3673

Sun JLXZZ, Liang H (2012) Parameterization of instantaneous global horizontal irradiance at the surface. Part II: cloudy-sky component. J Geophys Res. doi:10.1029/2012JD017557

Taylor KE (2001) Summarizing multiple aspects of model performance in a single diagram. J Geophys Res 106(D7):7183–7192

Thatcher M, McGregor JL (2009) Using a scale-selective filter for dynamical downscaling with the conformal cubic atmospheric model. Mon Weather Rev 137(6):1742–1752

Trigo ea R (2006) Relations between variability in the mediterranean region and mid-latitude variability. In: Lionello P, Malanotte-Rizzoli P, Boscolo R (eds) Mediterranean climate variability. Elsevier, Amsterdam, pp 179–226

Van Haren R, Van Oldenborgh G, Lenderink G, Collins M, Hazeleger W (2012) Sst and circulation trend biases cause an underestimation of european precipitation trends. Clim Dyn. doi:10.1007/s00382-012-1401-5

Van Oldenborgh G, Doblas-Reyes F, Wouters B, Hazeleger W (2012) Decadal prediction skill in a multi-model ensemble. Clim Dyn 38:1263–1280

Vidard PA, Dimet FXL, Piacentini A (2003) Determination of optimal nudging coefficients. Tellus A 55:1–15

Waldron KM, Paegle J, Horel JD (1996) Sensitivity of a spectrally filtered and nudged limited-area model to outer model options. Mon Weather Rev 124:529–547

Weisse R, Feser F (2003) Evaluation of a method to reduce uncertainty in wind hindcasts performed with regional atmosphere models. Coastal Eng 48:211–255

Xoplaki E, J GRJL, Wanner H (2004) Wet season mediterranean precipitation variability: influence of large-scale dynamics and trends. Clim Dyn 23:63–78

Xu Z, Yang Z (2012) An improved dynamical downscaling method with gcm bias corrections and its validation with 30 years of climate simulations. J Clim. doi:10.1175/JCLI-D-12-00005.1

Yong LI, Richard Ménar D, Lars Peter Riishøjgaar D, Cohn SE, Rood RB (1998) A study on assimilating potential vorticity data. Tellus A 50:490–506

Zampieri M, D'Andrea F, Vautard R, Ciais P, de Noblet-Ducoudré N, Yiou P (2009) Hot european summers and the role of soil moisture in the propagation of mediterranean drought. J Clim 22:4747–4758